J|A|C|S ARTICLES

Published on Web 04/06/2009

"Molecular Basket" Sorbents for Separation of CO_2 and H_2S from Various Gas Streams

Xiaoliang Ma,* Xiaoxing Wang, and Chunshan Song*

Clean Fuels and Catalysis Program, EMS Energy Institute and Department of Energy and Mineral Engineering, The Pennsylvania State University 209 Academic Projects Building, University Park, Pennsylvania 16802

Received September 18, 2008; E-mail: mxx2@psu.edu (X.M.); csong@psu.edu (C.S.)

Abstract: A new generation of "molecular basket" sorbents (MBS) has been developed by the optimum combination of the nanoporous material and CO_2/H_2S-philic polymer sorbent to increase the accessible sorption sites for CO_2 capture from flue gas (Postdecarbonization), and for CO_2 and H_2S separation from the reduced gases, such as synthesis gas, reformate (Predecarbonization), natural gas, coal/biomass gasification gas, and biogas. The sorption capacity of 140 mg of CO_2/g of sorb was achieved at 15 kPa CO_2 partial pressure, which shows superior performance in comparison with other known sorbents. In addition, an exceptional dependence of MBS sorption performance on temperature for CO_2 and H_2S was found and discussed at a molecular level via the computational chemistry approach. On the basis of the fundamental understanding of MBS sorption characteristics, an innovative sorption process was proposed and demonstrated at the laboratory scale for removing and recovering CO_2 and H_2S, respectively, from a model gas. The present study provides a new approach for development of the novel CO_2/H_2S sorbents and may have a major impact on the advance of science and technology for CO_2/H_2S capture and separation from various gases.

1. Introduction

The rapidly increasing concentration of greenhouse gas CO_2 in the atmosphere has caused serious concern for the global climate change. Carbon capture and sequestration (CCS) is considered one of the key options for mitigating the greenhouse gas emissions.[1−4] CO_2 can be captured from flue gas (Postdecarbonization),[5] separated from synthesis gas, coal/biomass gasification gas, and reformate (Predecarbonization),[6] or even captured from atmospheric air (Air-decarbonization).[7] In the production of hydrogen,[8−11] green synfuel,[6,12] city gas, and biomethane, one of the major processes is to separate and remove CO_2 and H_2S from the reduced gases, such as synthesis gas, reformate, natural gas, biogas, coal/biomass gasification gas, and others. In addition to the greenhouse effect of CO_2, the presence of CO_2 in the product hydrogen and fuel gas reduces significantly the energy content of the gas and lowers the efficiency in the transportation, storage, and application of the product hydrogen and fuel gas. H_2S is corrosive to equipment and pipelines as well as poisonous to the downstream catalysts and electrode catalysts in the solid oxide fuel cell (SOFC) and proton-exchange membrane fuel cell (PEMFC).[8,13] In both CCS and the hydrogen/green-synfuel production, one of the great challenges is to separate CO_2 from flue gas or separate CO_2 and H_2S from various process gases more economically and energy efficiently.

Amine scrubbing is a dominant technology currently used in industry for removing CO_2 and H_2S from various gas streams, as the amine solution has a higher capacity and selectivity for removing acidic gases. However, there are some major problems in this process: (1) high energy consumption, (2) low absorption/desorption rate, resulting in a larger size scrubber for increasing the gas−liquid interface,[14] (3) the solvent loss due to the degradation and evaporation in the process, (4) material corrosion due to the liquid amine solution, and (5) difficulty in removing sulfur to the level required for the fuel cell applications. On the basis of conventional technologies, the cost for CO_2 capture and separation from flue gas (Postdecarbonization) is estimated to represent three-fourths of the total cost of a carbon capture, storage, transport, and sequestration system. Consequently, it is highly desired to develop a novel sorbent material and a process with a high capacity, high selectivity, high regenerability, and high energy efficiency for separation of CO_2 and H_2S from various gas streams for CO_2 capture and for hydrogen, synfuel, and biomethane production.[15]

(1) Song, C. S. *Catal. Today* **2006**, *115*, 2.
(2) White, C. M.; Strazisar, B. R.; Granite, E. J.; Hoffman, J. S.; Pennline, H. W. *J. Air Waste Manage. Assoc.* **2003**, *53*, 645.
(3) Aaron, D.; Tsouris, C. *Sep. Sci. Technol.* **2005**, *40*, 321.
(4) Riahi, K.; Rubin, E. S.; Taylor, M. R.; Schrattenholzer, L; Hounshell, D. *Energiagazdalkodas* **2004**, *26*, 539.
(5) Service, R. F. *Science* **2004**, *305*, 962.
(6) Kintisch, E. *Science* **2008**, *320*, 306.
(7) Stolaroff, J. K.; Keith, D. W.; Lowry, G. V. *Environ. Sci. Technol.* **2008**, *42*, 2728.
(8) Song, C. S. *Catal. Today* **2002**, *77*, 17.
(9) Ritter, J. A.; Ebner, A. D. *Sep. Sci. Technol.* **2007**, *42*, 1123.
(10) Ni, M.; Leung, D. Y. C.; Leung, M. K. H.; Sumathy, K. *Fuel Process. Technol.* **2006**, *87*, 461.
(11) Haryanto, A.; Fernando, S; Murali, N.; Adhikari, S. *Energy Fuels* **2005**, *19*, 2098.
(12) Tilman, D.; Hill, J.; Lehman, C. *Science* **2006**, *314*, 1598.
(13) Farrauto, R.; Hwang, S.; Shore, L.; Ruettinger, W.; Lampert, J.; Giroux, T.; Liu, Y.; Ilinich, O. *Annu. Rev. Mater. Res.* **2003**, *33*, 1.
(14) Seader, J. D.; Henley, E. J. *Separation Process Principles*; John Wiley & Sons: 1998.

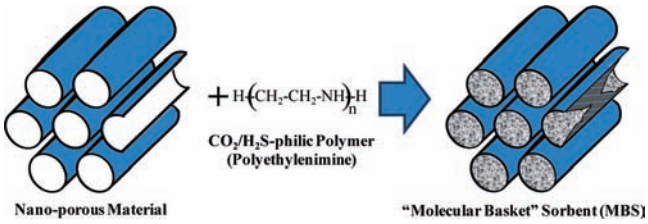

Figure 1. Principle for preparation of "molecular basket" sorbent (MBS).

In our previous study, we have developed a novel nanoporous material-supported polymer sorbent, called a "molecular basket" sorbent (MBS), for CO_2 capture from flue gas[16−19] and for H_2S removal from fuel gas.[20,21] As shown in Figure 1, the idea is to load a CO_2/H_2S-philic polymer sorbent, polyethylenimine (PEI), on the nanoporous material, such as MCM-41, to increase the accessible sorption sites per weight/volume unit of sorbent, and to improve the mass transfer rate in the sorption/desorption process by increasing the gas−PEI interface. Our previous study has indicated that MBS has some potential advantages, including a higher capacity (90 mg-CO_2/g-sorb at a CO_2 partial pressure of 15 kPa),[16] higher selectivity ($CO_2/N_2 > 1000$),[17] no corrosion as MBS is a solid, easy regeneration (at 100 °C),[16,18,20] positive effect of moisture on sorption capacity for both CO_2 and H_2S,[18,21] and high sorption/desorption rate.[17,20] It is because MBS combines the merits of both the solid nanoporous material and the polymer sorbent as well as both the adsorbent and the absorbent, which increases greatly the accessible sorption sites on/in the sorbent and improves the mass transfer in the sorption/desorption process.

As a part of our continuous effort in the development of MBS for CO_2 capture from flue gas and CO_2/H_2S removal from various fuel gases, we have made some significant progress in the present work in increasing the sorption capacity, finding an exceptional dependence of MBS on temperature for CO_2 and H_2S competitive sorption which has not been reported in the available literature to the best of our knowledge, and developing an innovative sorption process for removing CO_2 and H_2S, respectively, from the gas streams on the basis of the fundamental understanding of the sorption mechanism.

2. Results and Discussion

2.1. Properties of New Generation of MBS. A new generation of MBS has been developed in our laboratory by loading 50 wt% of polyethylenimine (PEI) on nanoporous SBA-15 (PEI/SBA-15), denoted as MBS-2. MBS-2 is different from the first generation of MBS (PEI/MCM-41), denoted as MBS-1, which was developed in our previous study by loading 50 wt% of PEI on MCM-41.[18,19] Some physical properties of MBS-2 and its support material SBA-15 are listed in Table 1 in comparison with those of MBS-1 and its support material MCM-41. MBS-1 had a BET surface area of 11 m^2/g with 97 v % of the pore volume filled by PEI, while MBS-2 had a BET surface area of 80 m^2/g, higher than that of MBS-1 by a factor of 7.3, with 85 v % of the pore volume filled by PEI, though both MBS-2 and MBS-1 had the same weight percent of the PEI loading. SEM images of MBS-2 presented in Figure 2 show that there are many large stacking (external) pores between the particles,[21] which facilitates the diffusion of the gas from the bulk of the gas phase to the surface of the sorbent. Both SEM and N_2 physisorption results indicate that the PEI was loaded inside the pore channels of the nanoporous material. In comparison with the typical absorber using the amine solution, a significant advantage of MBS-2 is the high surface area (80 m^2/g of sorb), which provides a gas−sorbent interface area of 4×10^7 square meter per cubic meter of the sorbent bed (m^2/m^3). This specific surface area is higher than that in the typical absorber in industry ($(2-3) \times 10^2$ m^2/m^3) by ∼5 orders of magnitude and higher than that of MBS-1 by more than 6 times. The high specific area can result in the high sorption−desorption rate with MBS-2, as the sorption−desorption rate per unit volume of sorber is directly proportional to the specific surface area.

Table 1. Physical Properties and Sorption Capacities of MBS-1, MBS-2, and Support Materials for CO_2 and H_2S, Respectively

sample	BET surface area (m^2 g^{-1})	pore volume (cm^3 g^{-1})	pore diameter (nm)	CO_2 cap.[a] mg/g of sorb	H_2S cap.[b] mg/g of sorb
MCM-41	1229	1.15	2.7	6.3	-
PEI(50)/MCM-41 (MBS-1)	11	0.03	0	89.2	62.6
SBA-15	950	1.31	6.6	5.0	0.034
PEI(50)/SBA-15 (MBS-2)	80	0.20	6.1	140	70

[a] Sorption at 75 °C and atmospheric pressure for a gas with 14.9 v % of CO_2 and 4.3% O_2 in N_2. [b] Sorption at 22 °C and atmospheric pressure for a gas with 4000 ppmv of H_2S and 20 v % of H_2 in N_2

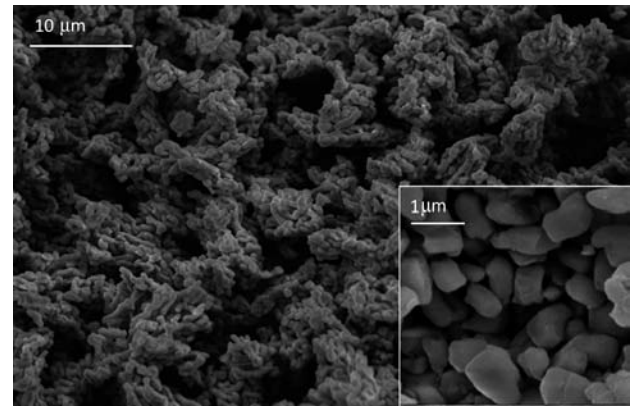

Figure 2. SEM images of MBS-2.

It should be highlighted that PEI is not simply loaded on MCM-41 and SBA-15 through only a physical interaction. Figure 3 shows the Diffused Reflectance Infrared Fourier Transform (DRIFT) spectra of SBA-15 and MBS-2 at room temperature in flowing N_2 with KBr as the background. Both of them were *in situ* pretreated in the DRIFT cell with flowing UHP N_2 at 75 °C for 2 h to ensure that it was "clean" prior to the IR study. Two sharp bands at 3747 and 1634 cm^{-1} and a broad band at ∼3500 cm^{-1} were observed over SBA-15, which can be assigned to hydrogen bonding in molecular H_2O and the H−O−H bend on SBA-15. After PEI loading, these bands either disappeared completely or were significantly reduced. The

(15) Service, R. F. *Science* **2004**, *305*, 963.
(16) Xu, X. C.; Song, C. S.; Andresen, J. M.; Miller, B. G.; Scaroni, A. W. *Energy Fuels* **2002**, *16*, 1463.
(17) Xu, X. C.; Song, C. S.; Andresen, J. M.; Miller, B. G.; Scaroni, A. W. *Microporous Mesoporous Mater.* **2003**, *62*, 29.
(18) Xu, X. C.; Song, C. S.; Miller, B. G.; Scaroni, A. W. *Ind. Eng. Chem. Res.* **2005**, *44*, 8113.
(19) Xu, X. C.; Song, C. S.; Miller, B. G.; Scaroni, A. W. *Fuel Process. Technol.* **2005**, *86*, 1457.
(20) Wang, X. X.; Ma, X. L.; Xu, X. C.; Sun, L.; Song, C. S. *Top. Catal.* **2008**, *49*, 108.
(21) Wang, X. X.; Ma, X. L.; Song, C. S. *Green Chem.* **2007**, *9*, 695.

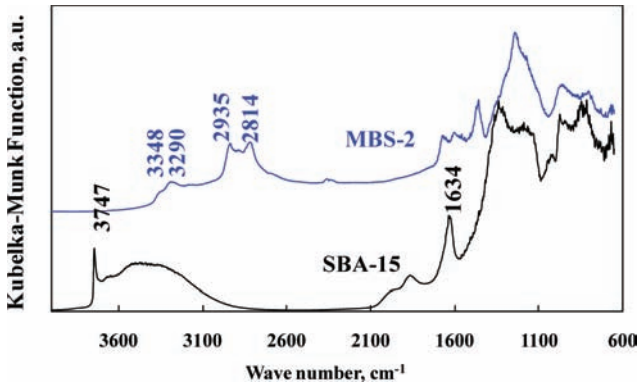

Figure 3. DRIFT spectra of SBA-15 and MBS-2 under N_2 atmosphere at 75 °C.

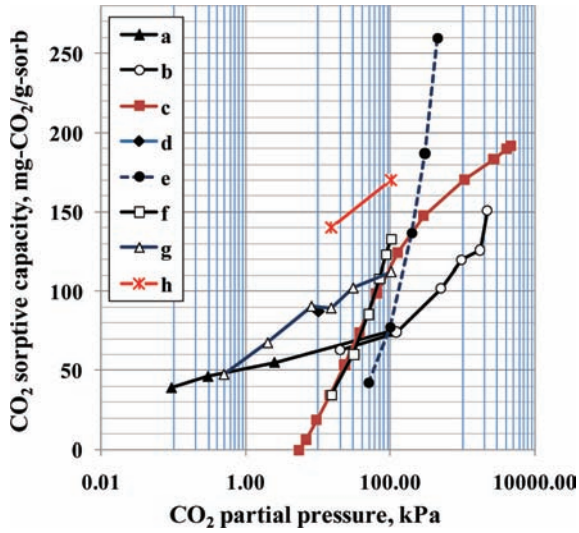

Figure 4. CO_2 sorption capacities of MBSs as a function of CO_2 partial pressure in comparison with some data reported in the literature for some typical commercial and developing absorbents and adsorbents. (a) 15 wt % MEA/H_2O at 40 °C by Austgen and Rochelle;[22] (b) 30 wt % DEA/H_2O at 40 °C by Rebolledo-Libreros and Trejo;[23] (c) 47 wt % MDEA/H_2O at 40 °C by Sidi-Boumedine et al.;[24] (d) SBA-HA at 75 °C by Hicks et al.;[25] (e) MOF-508b at 30 °C by Bastin et al.;[29] (f) ZIF-69 at 0 °C by Banerjee et al.;[27] (g) MBS-1 at 75 °C; (h) MBS-2 at 75 °C.

results suggest that there is a chemical interaction between the silanol groups on the surface of SBA-15 and the amine groups in PEI, which may form $Si-O^-N^+H_3R$ and/or $Si-O^-N^+H_2R$. Such chemical interaction works as an anchor to the PEI molecules on the surface of SBA-15 and keeps PEI in the pore channel, resulting in an increase of the thermal stability of the sorbent and decrease of the fluidity of PEI on the surface.

2.2. Sorption Capacity of MBS-2. The sorption of CO_2 on MBS-2 was conducted in a fixed-bed flow system at a temperature range from 22 to 100 °C. It was found that MBS-2 at 75 °C gave the highest capacity, as also observed for MBS-1.[16] The measured sorption capacities of MBS-2 at 75 °C as a function of CO_2 partial pressure are shown in Figure 4, in comparison with our previous results for MBS-1 and the data reported in the literature for some commercial and laboratory sorbents. The sorption capacity of MBS-2 is significantly higher than those of MBS-1[16] and the state-of-the-art absorbents and adsorbents. MBS-2 gave a sorption capacity of 140 mg of CO_2/g of sorb at 75 °C under a CO_2 partial pressure of 15 kPa, which is a typical value corresponding to the CO_2 partial pressure in flue gas (~15 vol% of CO_2). This capacity value is ~50% higher than that of MBS-1, more than 100% higher than the saturation absorption capacity of the 15 wt% MEA aqueous solution[22] and 30 wt% DEA aqueous solution,[23] and more than 300% higher than the saturation absorption capacity of the 47 wt% MDEA aqueous solution[24] at the same partial pressure. The capacity of MBS-2 is higher than that of the hyperbranched aminosilica sorbent (SBA-HA), reported recently by Hicks et al.,[25] by ~50%, as MBS-2 has an amine group density of ~12.3 mmol/g of sorb, which is higher than that (7.0 mmol/g of sorb) of SBA-HA by a factor of 1.8. At the CO_2 partial pressure of 15 kPa, the weight-based capacity of MBS-2 is higher than that of the state-of-the-art material zeolitic imidazolate frameworks (ZIF-69)[26,27] by a factor of 4 and of the metal-organic framework (MOF)[28,29] by a factor of even more than 4, as shown in Figure 4. To the best of our knowledge, MBS-2 has the highest weight-based CO_2 capacity at the partial pressure range from 10 to 100 kPa and the comparable temperature range in all state-of-the-art sorption materials reported in the literature.

The sorptive removal of H_2S by using MBS-1 and MBS-2 was also conducted in the fixed-bed flow system at a temperature range from 22 to 100 °C. Different from the CO_2 sorption, both MBS-1 and MBS-2 at 22 °C gave the highest H_2S sorption capacity in the temperature range examined.[18] Before the breakthrough, the H_2S concentration at the outlet was less than 60 ppbv, which was the H_2S detection limit of the instrument employed in our laboratory, indicating that both MBS-1 and MBS-2 are capable of removing H_2S at least to a level of 60 ppbv, which can meet the stringent requirement for the fuel cell applications. The measured saturation sorption capacities of MBS-1 and MBS-2 at 22 °C as a function of H_2S partial pressure are shown in Figure 5 in comparison with 50 wt % MDEA aqueous solution[30] and methanol[31] reported in the literature. MBS-2 gave a sorption capacity of 70 mg of H_2S/g of sorb at a H_2S partial pressure of 0.4 kPa. This value is ~12% higher than that of MBS-1, ~6.7 times higher than that of the 50 wt% MDEA aqueous solution, and ~10 times higher than that of methanol at the same H_2S partial pressure.

It is interesting to note that the sorption capacity of MBS-2 for CO_2 is higher than that of MBS-1 by 50%, although the loading amount of PEI in MBS-1 and MBS-2 is the same. It indicates that the support material plays an important role in determining the sorption performance. By comparison of the difference in the physical properties between the two support materials, a much higher capacity of MBS-2 than MBS-1 may be ascribed to the two factors of the support materials: (1) the pore diameter of SBA-15 is approximately twice that of MCM-41, and (2) the pore volume of SBA-15 (1.31 cm^3/g) is higher than that of MCM-41 (1.15 cm^3/g) by ~14%, which allows the MBS-2 prepared from SBA-15 to have a higher surface area

(22) Austgen, D. M.; Rochelle, G. T. *Ind. Eng. Chem. Res.* **1991**, *30*, 543.
(23) Rebolledo-Libreros, M. E.; Trejo, A. *Fluid Phase Equilib.* **2004**, *218*, 261.
(24) Sidi-Boumedine, R.; Horstmann, S.; Fischer, K.; Provost, E.; Fürst, W.; Gmehling, J. *Fluid Phase Equilib.* **2004**, *218*, 85.
(25) Hicks, J. C.; Drese, J. H.; Fauth, D. J.; Gray, M. L.; Qi, G.; Jones, C. W. *J. Am. Chem. Soc.* **2008**, *130*, 2902.
(26) Service, R. F. *Science* **2008**, *319*, 893.
(27) Banerjee, R.; Phan, A.; Wang, B.; Knobler, C.; Furukawa, H.; O'Keeffe, M.; Yaghi, O. M. *Science* **2008**, *319*, 939.
(28) Walton, K. S.; Millward, A. R.; Dubbeldam, D.; Frost, H.; Low, J. J.; Yaghi, O. M.; Snurr, R. Q. *J. Am. Chem. Soc.* **2008**, *130*, 406.
(29) Bastin, L.; Bárcia, P. S.; Hurtado, E. J.; Silva, J. A. C.; Rodrigues, A. E.; Chen, B. *J. Phys. Chem. C* **2008**, *112*, 1575.
(30) Huttenhuis, P. J. G.; Agrawal, N. J.; Hogendoorn, J. A.; Versteeg, G. F. *J. Petrol. Sci. Eng.* **2007**, *55*, 122.
(31) Fischer, K.; Chen, J.; Petri, M.; Gmehling, J. *AIChE J.* **2002**, *48*, 887.

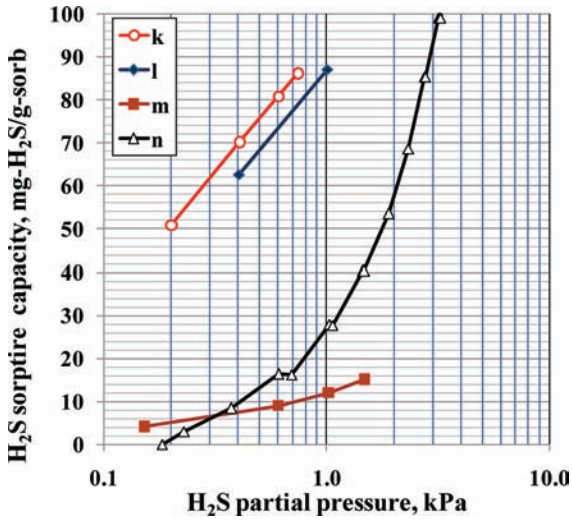

Figure 5. H_2S sorption capacities of MBSs as a function of H_2S partial pressure in comparison with data reported in the literature for some typical commercial absorbents. (k) MBS-2 at 22 °C; (l) MBS-1 at 22 °C; (m) 50 wt % MDEA/H_2O at 25 °C by Huttenhuis et al.;[30] and (n) MeOH at 25 °C by Fischer et al.[31]

than that from MCM-41 after the same PEI loading (50 wt %), as shown in Table 1. Both higher surface area and larger pore diameter of SBA-15 may significantly increase the total number of the accessible sorption sites in MBS-2 and thus enhance the CO_2 mass transfer in the sorption process. It should be pointed out that using SBA-15 as a support improved the sorption capacity of CO_2 more significantly than that of H_2S, indicating that the diffusion barrier of CO_2 in the bulk of PEI held in the pores may be higher than that of H_2S, which will be further discussed below via the computational chemistry approach.

The effect of the moisture in the gas on the sorption capacity for CO_2 is another important issue that needs to be clarified. The moisture effect on the sorption capacity of MBS-2 for CO_2 was examined by adding 3.0 v% of H_2O into a simulated flue gas with 15 v% of CO_2 and 4.5 v% O_2 in N_2. It was found that the presence of 3.0 v% of H_2O increased the saturation capacity of MBS-2 for CO_2 sorption by ~35%, which is consistent with our previous finding for MBS-1.[18] The result further confirms that the presence of the moisture in the gas has a promoting effect on the sorption capacity of MBS for CO_2.

2.3. Regenerability and Stability of MBS-2. For practical application, the sorbent should not only possess a high sorption capacity and high selectivity but also have excellent regenerability and stability in the sorption−desorption cycles. Using a TPD technique, 20 cycles of sorption−desorption experiment were carried out. Figure 6 shows the measured sorption capacity of MBS-2 for CO_2 as a function of the number of the sorption−desorption cycles. During the 20 cycles, the CO_2 sorption capacity of MBS-2 was kept at ~170 mg of CO_2/g of sorbent at the CO_2 partial pressure of 100 kPa, and no significant change in the CO_2 sorption capacity was observed. The desorption can be conducted by increasing the temperature to 110 °C, and the sorption capacity of the spent MBS-2 can be recovered completely after the regeneration, which is consistent with those observed in our previous studies in the regeneration of MBS-1 for CO_2 sorption[16,18] and the regeneration of MBS-2 for H_2S sorption.[20] It should be mentioned that in our preliminary experiment we have found that the coexisting SO_x and NO_x in the real flue gas caused the degradation of MBS-2 due to formation of the heat stable amine salts with PEI in MBS-2, as

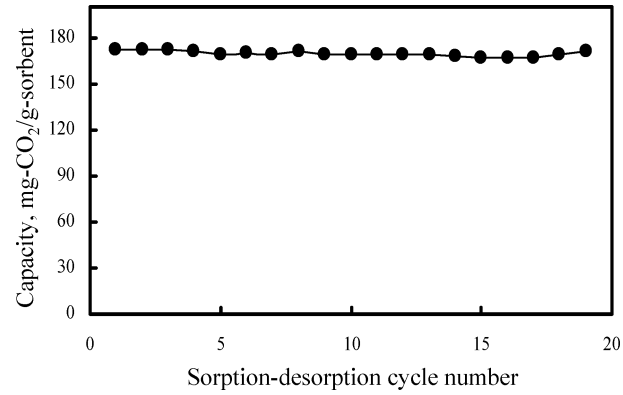

Figure 6. CO_2 sorption capacity versus the number of the sorption−desorption cycles over MBS-2 measured by TPD method. The CO_2 sorption was performed at 75 °C under a pure CO_2 flow for ~30 min. The desorption was carried out at 110 °C under a helium flow at a rate of 5 °C/min for 20 min.

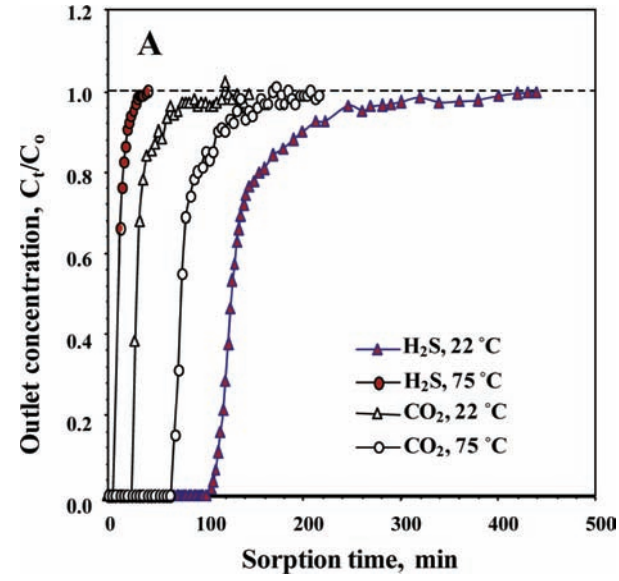

Figure 7. Sorption breakthrough curves for CO_2 and H_2S in single-stage sorption process using a model gas with 1.00 v% of CO_2 or 1.00 v% of H_2S in N_2 over MBS-1.

also observed in the sorption−desorption of CO_2 over MBS-1 using real flue gas.[18] It implies that the strong acidic gases, SO_2 and NO_2, need to be removed when using MBS-2 for CO_2 capture from flue gas, which is the same as that in the amine scrubbing process.

2.4. Dependence of MBS Sorption Performance on Temperature. Figure 7 shows the breakthrough curves on MBS-1 for CO_2 and H_2S, respectively, at 22 and 75 °C under a gas hourly space velocity (GHSV) of 1011 h^{-1} in a fixed-bed flow system using a model gas containing CO_2 or H_2S in N_2. For CO_2 removal, the sorption at 75 °C gave a much higher sorption capacity (70.8 mg of CO_2/g of sorb) than that at 22 °C (27.7 mg of CO_2/g of sorb). In distinct contrast, H_2S sorption at 22 °C gave a significantly higher sorption capacity (87.0 mg of H_2S/g of sorb) than that at 75 °C (7.8 mg of H_2S/g of sorb). These results clearly revealed the significant differences in the temperature dependences of MBS-1 for CO_2 and H_2S sorption, respectively. In many practical cases, CO_2 and H_2S coexist in the gas streams, such as fuel gas, syngas, and biogas. To clarify whether the presence of CO_2 in the gas streams inhibits the sorption of H_2S on the sorbent, a sorption experiment with a

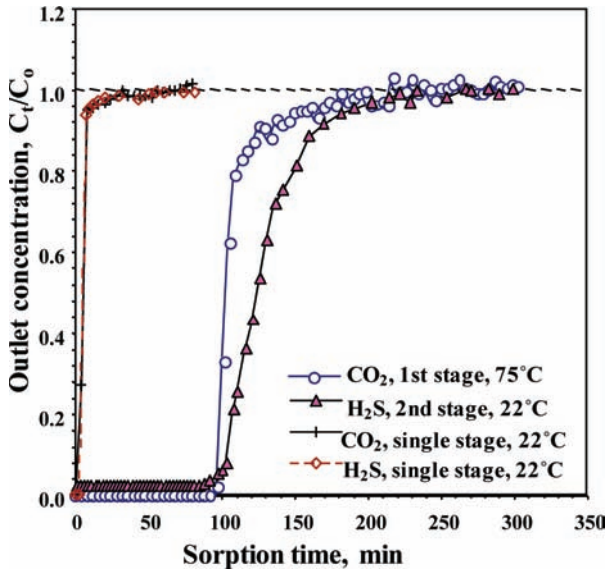

Figure 8. Sorption breakthrough curves for CO_2 and H_2S in single stage and two-stage sorption processes using a model gas containing 0.40 v% H_2S, 2.40 v% CO_2, and 20 v% H_2 in N_2 over MBS-1.

model gas containing 0.40 v % of H_2S, 2.40 % of CO_2, and 20 v % of H_2 in N_2 was performed at 22 °C and 1011 h^{-1} of GHSV. It was found that at this condition both CO_2 and H_2S broke through at the beginning, as shown in Figure 8, indicating that MBS-1 failed to remove H_2S and/or CO_2 at this condition.

The questions that arose are why does MBS-1 performance show a varying dependence on operating temperature for CO_2 and H_2S, why does MBS-1 have a lower sorption capacity for CO_2 than that for H_2S at 22 °C but shows the opposite trend at 75 °C, and why does the presence of CO_2 strongly inhibit the sorption of H_2S at 22 °C. To answer these questions, a computational study was conducted by using a semiempirical quantum chemical calculation method. It was hypothesized that the sorption of CO_2 or H_2S on MBS involves two steps: the adsorption of CO_2 or H_2S on surface of PEI and the diffusion of the adsorbate from the surface into the bulk of PEI in pores. The thermodynamic parameters of the heat of adsorption on the PEI surface and kinetic barrier of the diffusion from site to site in the PEI bulk for both CO_2 and H_2S were estimated, respectively, by semiempirical calculations. The results show that there are two types of sorption sites (site-I and site-II) for both CO_2 and H_2S sorption on PEI. The adsorption conformations of CO_2 and H_2S on site-I and site-II are shown in Figure 9. On site-I, the H_2S molecule interacts with a nitrogen atom in the amine group through the H atoms in H_2S, while the CO_2 molecule interacts with the nitrogen atom through the C atom in CO_2. On site-II, sorption of H_2S molecule is through an interaction of the two H atoms in H_2S, simultaneously, with two N atoms in two amine groups (in two neighboring PEI chains), while sorption of CO_2 is through an interaction of the C atom in CO_2 with the two N atoms simultaneously in two amine groups. The relative sorption heat of CO_2 and H_2S and the diffusion barrier in the bulk of PEI are shown in Figure 10. The results indicate that the heat of adsorption for CO_2 on the amine group is higher than that for H_2S, as CO_2 has stronger acidity than H_2S, which is consistent with the experimental heat of absorption in the amine solution reported in the literature.[32]

(32) Posey, M. L.; Rochelle, G, T. *Ind. Eng. Chem. Res.* **1997**, *36*, 3944.

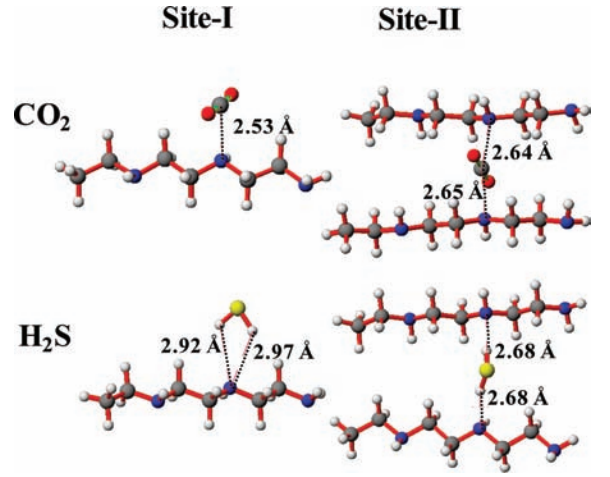

Figure 9. Computationally optimized sorption conformation of CO_2 and H_2S on Site-I and Site-II in PEI.

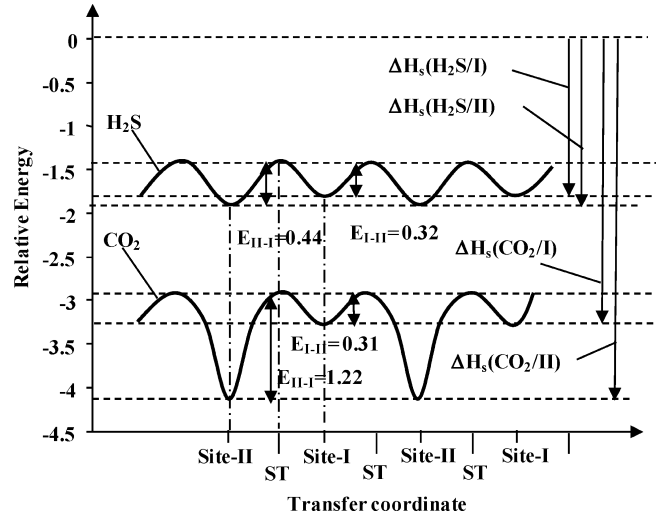

Figure 10. Potential energy surface for sorption and transfer of CO_2 and H_2S on Site-I and Site-II in PEI.

It implies that the thermodynamics favors the adsorption of CO_2 on the PEI surface more than that of H_2S. On the other hand, it is of interest to note that the estimated kinetic barrier for diffusion of the sorbed CO_2 from the surface into the bulk of PEI is higher than that for diffusion of the sorbed H_2S by a factor of ~3, indicating that the diffusion of the sorbed CO_2 from the exposed surface of PEI into the bulk of PEI is much more difficult than that of the sorbed H_2S.

On the basis of the computational results, the lower CO_2 sorption capacity at 22 °C than that at 75 °C can be ascribed to the higher kinetic barrier for diffusion of the CO_2 sorbed from the surface into the bulk of PEI, which reduces significantly the total number of the accessible sorption sites for CO_2 at 22 °C, although low temperature thermodynamically favors the adsorption of CO_2 on the surface of PEI. The increase in temperature facilitates the transfer of the adsorbed CO_2 molecules from the surface into the bulk of PEI by overcoming the kinetic barrier. This leads to a significant enhancement of the total number of the accessible sorption sites at 75 °C, although the increase in temperature does not favor thermodynamically the sorption of CO_2 on the surface and in the bulk of PEI. On the other hand, the higher heat of sorption for CO_2 makes the sorption affinity at 75 °C high enough to capture CO_2. As a

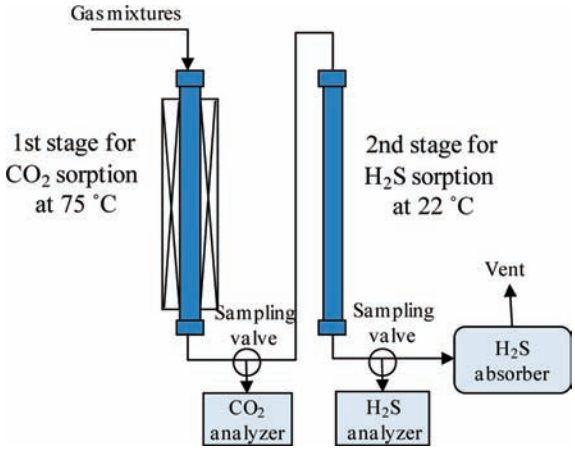

Figure 11. Scheme of the experimental two stage process for removal of CO_2 and H_2S from a model fuel gas. Inlet gas: 0.40 v % H_2S, 2.40% CO_2, and 20% H_2 in N_2; sorbent in both the first and second stages: MBS-1.

result, MBS-1 exhibited a higher sorption capacity for CO_2 at 75 °C than at 22 °C. A further increase of temperature above 75 °C reduces the CO_2 sorption capacity, as the control of the sorption shifts from the kinetic regime to the thermodynamic regime.

For sorption of H_2S, due to a lower kinetic barrier for the transfer of the sorbed H_2S in the bulk of PEI, the H_2S molecules adsorbed on the surface are easier to diffuse into the PEI bulk even at 22 °C. On the other hand, the lower temperature thermodynamically favors the increase in the equilibrium sorption capacity. Consequently, MBS-1 exhibited a higher sorption capacity for H_2S at 22 °C than at 75 °C. Due to the significantly higher heat of sorption for CO_2 than for H_2S, the coexisting CO_2 molecules preferentially occupy the sorption sites on the surface and, thus, block the way for sorption of H_2S on the surface, as indicated in Figure 8. Both the thermodynamic and kinetic factors work together to determine the exceptional dependence of MBS performance on temperature for CO_2 and H_2S sorption. The higher kinetic diffusion barrier for CO_2 than for H_2S also explains why the sorption performance of MBS-2 is much better than that of MBS-1 for CO_2, but the sorption performance of both are almost the same for H_2S. It is probably because for CO_2 sorption, but not for H_2S sorption, the diffusion is a primary factor that affects the total number of the accessible sorption sites, and the higher surface area of MBS-2 and larger pore diameter of SBA-15 in MBS-2 facilitate the diffusion of CO_2 in MBS-2.

2.5. Two-Stage Process for Respective Removal of CO_2 and H_2S. On the basis of the fundamental understanding of the sorption mechanism, a novel two-stage sorption process was proposed with two sorption beds in series for removing CO_2 and H_2S, respectively, from gas streams. The two-stage process was demonstrated in our laboratory by using MBS-1 and a model gas with 0.40 v % of H_2S, 2.40 v % of CO_2, and 20 v % of H_2 in N_2 gas at a flow rate of 60 mL/min. A scheme of the experimental two-stage process is shown in Figure 11. The first stage with MBS-1 as a sorbent was operated at 75 °C for removing CO_2, and the second stage with the same sorbent at room temperature (22 °C) for removing H_2S. The CO_2 concentration at the outlet of the first stage and the H_2S concentration at the outlet of the second stage as a function of time are plotted in Figure 8, for comparison. In the first stage, the CO_2 breakthrough time was ~95 min, corresponding to a breakthrough capacity of 80 mg of CO_2/g of sorb, indicating that the sorption of CO_2 at 75 °C is not affected by the coexistence of H_2S, as expected. In the second stage, the H_2S breakthrough time was ~95 min, corresponding to a capacity of 19 mg of H_2S/g of sorb. This value was lower than the expected one, because the CO_2 that had broken through in the first sorption bed entered the second sorption bed and inhibited the H_2S sorption in the second bed, resulting in the early H_2S breakthrough in the second bed. The results clearly show that the two-stage process successfully removed CO_2 and H_2S, respectively, from the simulated fuel gas. It indicates that the developed process has a potential and wide application in the cleanup of the reduced gases, including hydrogen, reformate, synthesis gas, natural gas, biogas, coal/biomass gasification gas, and others.

3. Concluding Remarks

In summary, a new generation of "molecular basket" sorbent, MBS-2, has been developed in our laboratory for CO_2/H_2S capture. MBS-2 gives a high sorption capacity of 140 mg of CO_2/g of sorb at 75 °C under 15 kPa CO_2 partial pressure, which is ~50% higher than that of the previously developed MBS (MBS-1). MBS-2 shows the highest CO_2 capacity under the CO_2 partial pressure range from 10 to 100 kPa in the comparable temperature range among all the commercial and state-of-the-art adsorbents, absorbents, and sorbents reported to date.

The exceptional dependence of MBS performance on temperature for CO_2 and H_2S sorption has been found and explained at a molecular level via the computational chemistry approach. On the basis of the new findings, an innovative two-stage process for removing CO_2 and H_2S, respectively, from gas streams was proposed and demonstrated in a laboratory apparatus. The sorbent and process developed in this work have many distinct advantages: (1) high sorption capacity and selectivity for CO_2 and H_2S, (2) capable of removing H_2S to less than 60 ppbv, (3) higher sorption−desorption rate due to higher gas−sorbent interface area, (4) good regenerability and stability in sorption−desorption cycles, (5) promoting effect of moisture in the gas on the sorption capacity, and (6) ability to remove and recover CO_2 and H_2S, respectively.

The present study provides a new approach for the development of novel sorbents by the combination of a solid nanoporous material and a polymer sorbent, of an adsorbent and an absorbent, and of inorganic and organic materials, which may have a major impact on the advance of science and technology for CO_2 capture from flue gas, CO_2/H_2S separation from various reduced gases, and other gas separation.

4. Experiment and Calculation Method

4.1. Preparation of MBS. MBS-1 and MBS-2 were prepared by loading polyethylenimine (PEI) on mesoporous molecular sieves MCM-41 and SBA-15, respectively, using a wet impregnation method. PEI used in the present study was a linear polymer, which was purchased from Aldrich with an average molecular weight of 423 g/mol, boiling point of ~250 °C, and viscosity of 200 cP at 25 °C. MCM-41 and SBA-15 were synthesized by a hydrothermal method. MCM-41 was synthesized from a mixture with the following composition: $50SiO_2/4.32Na_2O/2.19(TMA)_2O/15.62CTAB/3165H_2O$, which was established in our laboratory,[33,34] based on the method invented by Mobil researchers.[35,36] The SBA-15 was

(33) Reddy, K. M.; Song, C. S. *Catal. Lett.* **1996**, *36*, 103.
(34) Reddy, K. M.; Song, C. S. *Stud. Surf. Sci. Catal.* **1998**, *117*, 291.
(35) Kresge, C. T.; Leonowicz, M. E.; Roth, W. J.; Vartuli, J. C.; Beck, J. S. *Nature (London)* **1992**, *359*, 301.

synthesized according to the procedure reported in the literature.[37,38] Typically, a homogeneous mixture, which was composed of triblock copolymer Pluronic P123 ($EO_{20}PO_{70}EO_{20}$, MW = 5800, Aldrich) and tetraethyl orthosilicate (TEOS) in hydrochloric acid, was stirred at 40 °C for 20 h and then further treated at 100 °C for 24 h. After the synthesis, the resultant solid was recovered by filtration, washed and dried at 100 °C overnight, and finally calcined at 550 °C for 6 h. The typical preparation methods of MBS-1 and MBS-2 were reported in detail in our previous paper.[20]

4.2. Characterization of Sorbents. The pore structure and surface area of the prepared MCM-41, SBA-15, MBS-1, and MBS-2 were characterized by adsorption/desorption of nitrogen at −196 °C using a Micromeritics ASAP2010 surface area and porosimetry analyzer. Standard BET and DR models were respectively applied to derive surface area and pore volume. The pore size distribution was calculated according to the Barrett−Joyner−Halenda (BJH) model.[39] The scanning electron microscopy (SEM) images were obtained on a Hitachi S-3500N instrument operating at 5 kV.

A Nicolet NEXUS 470 FT-IR spectrometer (Thermo Electron Corp.) was used to obtain the DRIFT Spectra of the SBA-15 and MBS-2 samples. The powder of each sample (∼20 mg) was placed into the DRIFT cell and pretreated in flowing UHP N_2 at 75 °C for 2 h. Then the DRIFT spectra were collected under N_2 atmosphere at 75 °C. KBr was used as the background at the same conditions. The IR resolution was 4 cm^{-1}.

4.3. Sorption Measurements. The sorption separation of CO_2 and/or H_2S from the model gases was performed in a fixed-bed flow sorber (straight glass tube with inner diameter of 9.5 mm) operated at atmospheric pressure. Special tubing and fittings coated with a sulfur inert material (purchased from Restek Corp.) were used for the sorption system to reduce the effect of adsorption of H_2S on the tubing wall. In a typical sorption process, ∼1.5 g of the sorbent was packed into the bed (bed length was ∼75 mm), and the empty spaces were filled with inert glass beads. Before the sorption test, the sorbent bed was heated to 100 °C in nitrogen at a flow rate of 100 mL/min and held overnight to desorb all presorbed species. Then, the sorbent bed was cooled down to room temperature, and the whole sorber was sealed and weighed to calculate the real weight of the used sorbent. After the sorber was connected back into the system, the sorbent bed was heated to the desired sorption temperature, and then, the model gas was introduced into the bed. The treated gas out of the sorber was analyzed online by using an SRI 8610C gas chromatograph with molecular sieve 5A and Porapak T columns and with a TCD detector (GC-TCD), and an ANTEK 9000NS Sulfur Analyzer, respectively, for CO_2 and H_2S. For the gas samples with H_2S concentration less than 1 ppmv, a gas detection system, Sensidyne/Gastec, was used. The saturation capacity, which was denoted as Cap, milligram of CO_2 or H_2S per gram of sorbent (mg/g of sorb), was calculated by using the following equation:

$$Cap = \frac{MW \times FR \times \int_o^t (C_o - C_t)\,\mathrm{d}t}{W_{sorb}} \qquad (1)$$

where t is the sorption time (min); FR is the flow rate (mmol/min); W_{sorb} is the weight of sorbent (g); MW is the molecular weight (g/mol) of CO_2 or H_2S; and C_o and C_t are the inlet and outlet concentration of CO_2 or H_2S.

4.4. Evaluation of Regenerability and Stability of MBS-2. The temperature-programmed desorption (TPD) method was used to measure the regenerability and stability of MBS-2 for CO_2 sorption. CO_2-TPD was conducted by using a Micromeritics AutoChem 2910 instrument with a TCD. MBS-2 (∼100 mg) was loaded into a U-shape quartz reactor and pretreated at 100 °C under pure helium for 30 min. Then the temperature was cooled down to 75 °C, and CO_2 sorption was performed at this temperature under a pure CO_2 flow for ∼30 min. After that, the temperature was decreased to room temperature under CO_2 flow. The desorption experiments were then carried out by passing helium through the tube and ramping the temperature from room temperature to 110 °C at a rate of 5 °C/min and holding at 110 °C for 20 min. The sorption capacity of the regenerated MBS-2 was measured on the basis of the amount of the desorbed CO_2. The same sorption−desorption procedure was conducted for 20 cycles to evaluate the regenerability and stability of MBS-2.

4.5. Computational Method. All quantum chemical calculations in this study were performed by means of the semiempirical PM5 method, using the CAChe program. To reduce the computational cost, a simple model (a trimer of ethylenimine (TEI)):

$$NH_2-CH_2-CH_2-NH-CH_2-CH_2-NH-CH_2-CH_3$$

which contains one primary amine group and two secondary amines, was used to mimic PEI. The adsorption conformations of CO_2 and H_2S on the secondary amine in TEI were optimized by the PM5 method. The pseudo heat of sorption was defined and estimated on the basis of the following equation:

$$\Delta H_{\mathrm{sorption}} = \Delta H^\circ_{\mathrm{f,TEI\text{-}sorbate}} - (\Delta H^\circ_{\mathrm{f,TEI}} + \Delta H^\circ_{\mathrm{f,sorbate}}) \qquad (2)$$

where $\Delta H^\circ_{\mathrm{f,TEI}}$ and $\Delta H^\circ_{\mathrm{f,sorbate}}$ are the heat of formation of TEI and sorbate, respectively. $\Delta H^\circ_{\mathrm{f,\ TEI\text{-}sorbate}}$ is the heat of formation of TEI-sorbate (heat of formation for whole TEI and sorbate after interaction). In the present study, we only examined the interaction between CO_2 (or H_2S) and the secondary amine group in PEI, as we used a linear PEI for preparing MBS-1 and MBS-2, which had a secondary-amine/primary-amine ratio of ca. 9 according to the average molecular weight.

The kinetic barrier (E_t) for transfer of the sorbed molecule from one sorption site to the other was estimated by finding the transition state and calculation according to the following equation:

$$E_t = \Delta H^\circ_{\mathrm{f,ST}} - \Delta H^\circ_{\mathrm{f,TEI\text{-}sorbate}} \qquad (3)$$

where, $\Delta H^\circ_{\mathrm{f,\ ST}}$ is the heat of formation of the transition state from one site to the other.

Acknowledgment. This study was supported in part by Pennsylvania Energy Development Authority through PA Department of Environmental Protection Grant PG050021, by the U.S. Office of Naval Research through ONR Grant N00014-08-1-0123, and by the U.S. Department of Energy, National Energy Technology Laboratory through DOE Grant DE-FC26-08NT0004396.

JA8074105

(36) Beck, J. S.; Vartuli, J. C.; Roth, W. J.; Leonowicz, M. E.; Kresge, C. T.; Schmitt, K. D.; Chu, C. T. W.; Olson, D. H.; Sheppard, E. W.; McCullen, S. B.; Higgins, J. B.; Schlenker, J. C. *J. Am. Chem. Soc.* **1992**, *114*, 10834.

(37) Zhao, D.; Feng, J.; Huo, Q.; Melosh, N.; Fredrickson, G. H.; Chmelka, B. F.; Stucky, G. D. *Science* **1998**, *279*, 548.

(38) Wang, X.; Zhang, Q.; Yang, S.; Wang, Y. *J. Phys. Chem. B* **2005**, *109*, 20835.

(39) Choma, J.; Jaroniec, M.; Kloske, M. *Sep. Sci. Technol.* **2002**, *20*, 307.